Rheological Characterization of Carbopol® Dispersions in Water and in Water/Glycerol Solutions

Priscilla R. Varges, Camila M. Costa, Bruno S. Fonseca, Mônica F. Naccache and Paulo R. de Souza Mendes *

Department of Mechanical Engineering, Pontifícia Universidade Católica-RJ, Rua Marquês de São Vicente 225, Rio de Janeiro, RJ 22453-900, Brazil; prvarges@puc-rio.br (P.R.V.); camila.moreira.costa@hotmail.com (C.M.C.); brunodasilva.fonseca@gmail.com (B.S.F.); naccache@puc-rio.br (M.F.N.)

* Correspondence: pmendes@puc-rio-br; Tel.:+5521-99982-9653

Abstract: The influence of the solvent type on the rheological properties of Carbopol® NF 980 dispersions in water and in water/glycerol solutions is investigated. The material formulation, preparation procedure, common experimental challenges and artifact sources are all addressed. Transient and steady-state experiments were performed. For both solvent types, a clearly thixotropic behavior occurs slightly above the yield stress, where the avalanche effect is observed. For larger stresses, thixotropy is always negligible. Among other findings, it is observed that, for a given Carbopol concentration, the dispersion in the more viscous solvent possesses a lower yield stress and moduli, a larger power-law index, and a longer time to reach steady state.

Keywords: Carbopol; yield stress; thixotropy

---

1. Introduction

Materials like colloidal suspensions, emulsions, foams, gels, and granular materials only flow irreversibly when a finite threshold shear stress—known as the *yield stress*—is exceeded [1–9].

Carbopol®, a trademark owned by Lubrizol Corporation (Wickliffe, OH, USA), is a family of commercial polymers frequently employed in the cosmetics, pharmaceutical, paint, and food industry as a thickening, suspending, dispersing, and stabilizing agent [10]. In research activities, its solutions are frequently employed in flow visualization experiments [11–14], because they are transparent gels that are relatively easy to prepare [15–17].

There are more than 10 grades of Carbopol polymers, which may be subdivided into several categories based on their physical structure and chemical composition, crosslink density, polymerization solvent, type of cross-linking, network electrical charge, and physical appearance [18]. Carbopol is a high molecular weight, hydrophilic, and crosslinked polyacrylic acid polymer. This physical hydrogel presents a three-dimensional polymer network that is swollen by water, and presents temporary, reversible interchain entanglements that are stronger when compared to chemical hydrogels.

Specifically, in the present research we employed Carbopol NF 980, also known as a monograph Carbomer Homopolymer Type C (former Carbomer 940) by U.S. Pharmacopeia/National Formulary (USP/NF) in the United States. Carbopol NF 980 is a synthetic homopolymer, polyacrylic acid crosslinked with allyl sucrose or allyl pentaerythritol, which is polymerized in a co-solvent system. It is supplied as a white and dry powder of primary particles averaging 0.2 μm in diameter. It is a weak anionic

polyelectrolyte polymer that must be neutralized in order to achieve a high viscosity. Each particle (or network structure) is a mixture of tightly coiled linear polymer chains, which are soluble in polar solvents. The viscosity of Carbopol solutions is not a function of the size of its powder particles [19].

It is well known that this polymer forms a colloidal dispersion when hydrated in water at controlled pH and temperature. Frequently, a Carbopol aqueous dispersion is neutralized with a common base, such as sodium hydroxide (NaOH), converting the acidic polymer into a salt. When neutralized, the polymer presents the ability to absorb and retain water. Polymer chains interconnected by crosslinks begin to hydrate, and partially uncoil due to electrostatic repulsion in order to form irreversible agglomerates [20]. The desired yield stress nature is due to the presence of high molecular weight polyacrylate branched chains that form interchain entanglements which prevent flow at low shear stresses [19,21,22]. During hydration the chains may increase up to 10 times their original diameter [23], and the ionization process leads to a crosslink of the swollen molecules, forming a microgel network with stronger bonds.

In order to better understand the rheological properties of Carbopol solutions, it is fundamental to improve the knowledge of their relation with the material microstructure [24]. Data obtained in rheological measurements are better interpreted when supported by visualization techniques such as microscopy, X-ray, neutron and light scattering, nuclear magnetic resonance (NMR) or differential scanning calorimetry (DSC) [25]. Indeed, Ref. [23] investigated Carbopol viscoelastic properties through direct analysis of the microscopic network structure by scanning electron cryomicroscopy (cryoSEM). Likewise, Ref. [26] studied elasticity through microrheology. On the other hand, Ref. [20] emphasized the need for novel microscopic scale experiments, that would be able to simultaneously describe local dynamics and flow behavior.

Steady and oscillatory simple shear flows provide information on the relationship between the rheological properties and the macromolecular structure. Viscoelastic effects are a result of the interaction between polymer chains that is related to the viscous behavior, and the chains recoiling due to thermal motion, which is related to the elastic behavior [27]. Colloidal dispersions such as Carbopol present a typical viscoelastic behavior at low stresses [28]. On the other hand, elastic effects decrease and eventually tend to become negligible at the higher stresses found in the nonlinear steady state.

The rheological properties of Carbopol dispersions have been extensively investigated [16,23,29–31]. These properties depend on the type and degree of crosslinking, which in turn depend on molecule swelling and medium density. Carbopol dispersion is usually seen as simple model yield stress fluids [32,33]. Their viscoplastic steady state behavior is well represented by the Herschel-Bulkley equation [34], which can accommodate a yield stress and a power-law shear-thinning behavior. However, for some soft glassy materials, other important features cannot be neglected, such as pronounced elastic and thixotropic behavior (especially when the stress is close to the yield stress), transient and initial internal stresses, normal stress differences, and irreversibility of the deformed states [9,32,35–37]. Ref. [38] argue that, at low stresses, the microgels do not move relatively to each other, but are able to deform, resulting in a solid-like elastic behavior. At large stresses, there is relative mobility of the microgels, leading to a liquid-like viscoelastic behavior.

Yield stress materials can be classified according to their microstructure as repulsive-dominated jammed glasses, networked gels with attractive interactions or a combination thereof [39,40]. According to [39], Carbopol gels are classified into the first category.

Ref. [16] describes Carbopol gels as concentrated, percolated, and disordered dispersions with glassy structure. Structural variations occur as the polymer concentration is increased. For $c < 0.035 \, \text{wt}\%$, the dispersion obtained possesses no yield stress; for $0.035 < c < 0.12 \, \text{wt}\%$ a percolated viscoelastic dispersion is obtained; for $0.12 < c < 0.21 \, \text{wt}\%$ the dispersion obtained is phase-inverted percolated with excess of solvent; and for $c > 0.21 \, \text{wt}\%$ a closely packed and disordered structure is observed, due to polydispersity.

Using confocal fluorescence microscopy, Ref. [17] observed that the Carbopol microgels are indeed polydisperse. They also observed that, at the same concentration, Carbopol Ultrez 10 and ETD 2050

(Lubrizol Corporation, Wickliffe, OH, USA) present the same mesostructure, despite a difference in particle size. The microgels have complex shape when unconstrained, and possess soft elasticity and capacity to adapt their outer shape and swelling ratio to local space and solvent availability conditions. In addition, the maximum volume concentration can be quite high due to the also high albeit as yet not quantified polydispersity.

For a 1.5 wt% concentration, Ref. [19] observed the existence of highly swollen deformable microgel particles closely packed and in intimate contact. The high viscosity is determined by network cross-link density, which governs particle-particle interaction. On the other hand, dilute dispersions, i.e., dispersions of fully swollen particles with no contact, the particle-solvent interactions result in lower viscosity and elasticity.

Carbopol dispersions show different behavior depending on the solvent [41]. In general, water is used as a solvent. However, co-solvent and anhydrous systems have also been used [42]. Ethanol and isopropanol can be thickened adding Carbopol polymers [43]. In this case, it is crucial to use the appropriate neutralizer, which varies depending upon the alcohol content. In addition, previous works have already demonstrated the possibility of formulating Carbopol systems using different hydrophilic solvents such as polyethylene glycol (PEG) 400, glycerol, silicone, and tetraglycol without neutralization [44].

The choice of the solvent is also important because solvents such as glycerol and propylene glycol can modify hydrogen bond characteristics between water, solvent, and polymer, thereby affecting polymer swelling and the viscoelastic properties [30,41,45].

The present research aims to explore the rheological properties of Carbopol NF 980 dispersions in different formulations. Solvent type, polymer concentration, gel preparation, mechanical properties, and phenomenological behavior are all discussed. We carried out systematic rheological experiments, in transient and steady state regimes, from which we observe that Carbopol gels are not as "simple" as usually assumed.

2. Experimental Protocol

2.1. The Carbopol

Carbopol NF 980 polymer presents a bulk density of 176 Kg/m^3 and in the crosslinked form shows a molecular weight as high as 4.5 billion due to the interlinkage of many polymer chains [46]. Ref. [10] estimated the Carbopol 940 molecular weight between crosslinks as 1.04×10^5, while [19] calculated 5×10^6. In general, all members of the Carbopol family possess a considerably high molecular weight.

2.2. Fluid Preparation

Carbopol aqueous and water/glycerol dispersions were prepared based on the procedures recommended by the manufacturer [43,45,47,48]. Weight concentrations ranging from 0.1 wt% to 0.15 wt% were investigated. All the water/glycerol solutions used as continuous phase were composed of 60% of glycerol and 40% of water, in volume.

Ref. [16] emphasized that a strict protocol for preparation of Carbopol dispersions is fundamental to achieve reproducibility. For the same concentration, he affirms that water properties, reagents involved, dispersion methods, and also the reservoir used during the mixing process can affect the dispersion properties. Therefore, its rheology is a function of concentration, composition, pH, temperature, aging and preparation procedure [31].

A detailed description of the dispersion preparation is now presented. Before preparation, it is important to sift the Carbopol dry powder through a 20-mesh metallic screen to eliminate aggregates which prevent complete hydration, severely affecting the quality of the dispersion.

A 6 L plastic vessel is used to prepare and store the dispersion. Initially, it is filled with a predetermined mass of water obtained from a reverse osmosis system. The vessel with water is placed on a mechanical stirrer equipped with a 3-blade marine impeller positioned close to vessel bottom. The stirrer is turned on at 1200 rpm. A cover is used to minimize solvent evaporation and contamination. Carbopol should be carefully and slowly added to the vessel, approximately halfway between the blade and the vessel wall, to avoid adhesion to solid surfaces.

For Carbopol aqueous dispersions, after polymer addition the agitation is maintained at 1200 rpm for 15 min and then kept at rest for 30 min. On the other hand, for dispersions of Carbopol in water/glycerol solutions, the water/glycerol solution is added after powder addition, with the mixer at 700 rpm. Stirring is applied for 15 min, and then the dispersion is kept at rest.

For both types of dispersion, the 3-blade marine impeller is then replaced by a naval blade and the mixer is set to 150 rpm, to minimize formation of air bubbles. A 18 wt% NaOH aqueous solution is then added to neutralize the dispersion.

Finally, for the aqueous dispersion, the agitation is increased to 300 rpm and maintained uninterruptedly for 5 days, to homogenize the dispersion. In the presence of glycerol, the agitation is kept at 150 rpm for 7 days. This final step is very important since we observed that longer mixing times favor reproducible data as they improve the complete process of hydration and material stability over time [31,49].

2.3. Rheological Measurements

The rheological properties of the Carbopol dispersions are measured using two stress-controlled rheometers, namely the AR-G2 and the DHR-3 by TA Instruments (New Castle, DE, USA). Both are combined motor and transducer (CMT) instruments. Instrument inertia is an important source of artifact, especially for low-viscosity liquids. Therefore, it is important to apply the suitable corrections [50–53].

The rheology of Carbopol dispersions depends very weakly on temperature [23,30]. Nevertheless, all tests were performed at 25 °C. A Peltier system was employed to control the sample temperature. Carbopol dispersions are volatile [15–17]. Therefore, to minimize evaporation and keep constant the shape of the free meniscus, a solvent trap with water was used to create a saturated atmosphere around the sample [54].

In general, the geometry selection is based on the characteristics of the material to be tested. Due to the yield stress, Carbopol dispersions tend to present apparent wall slip at low strain rates [55–57], as usually observed in structured materials. Therefore, roughened surfaces are in order. The plate-plate geometry is usually preferred for dispersions as opposed to the cone-plate geometry, to ensure that the minimum gap throughout the sample is about 10 times the characteristic size of the dispersed phase [54]. In the present research, a 60 mm diameter cross-hatched plate-plate geometry with a 1 mm gap was used in the tests. This geometry was made of titanium, which has the advantage of preventing chemical attacks and minimizing instrument inertia.

A disadvantage of the plate-plate geometry is the flow inhomogeneity, in the sense that the shear rate throughout the sample is not uniform. Rather, it varies linearly with the radial position, and hence for non-Newtonian liquids the viscosity also varies with the radial position. For steady flow, the Weissenberg-Rabinowitsch equation circumvents this problem by giving the shear stress at the rim [58]. A similar treatment was proposed by [59] to evaluate the stress amplitude at the rim for oscillatory flows. For creep (viscosity or shear-rate bifurcation) tests, no correction is needed, because the material behaves as a solid below the yield stress [59].

With the aid of a glass syringe, the sample is positioned at the center of the bottom plate. Carbopol dispersions tend to retain bubbles [15–17]. If bubbles are trapped during loading, they should be removed

by suction with a needle syringe. Then the upper plate is positioned slightly above its final position, and the sample excess is trimmed. The upper plate is then brought to the measuring position, the free surface at the rim is checked for irregularities, and the solvent trap is positioned.

Before the beginning of the test, the sample is kept at rest for 30 min to allow for thermal equilibrium and rebuilding of the microstructure which is partially broken during loading. Ref. [60] argues that the resting time essentially eliminates residual stresses.

To verify repeatability, the tests should be repeated at least once, always with a fresh sample.

3. Results and Discussion

3.1. Stress Amplitude Sweep Tests

Typical results for a stress amplitude sweep test are presented in Figure 1. The material is a 0.123 wt% Carbopol aqueous dispersion, and the frequency was kept fixed at 1 Hz. In this figure, the storage modulus G', loss modulus G'', and complex modulus G^* are given as a function of the imposed shear stress amplitude, τ_a. Instrument inertia [61] and flow inhomogeneity [59] effects are corrected for.
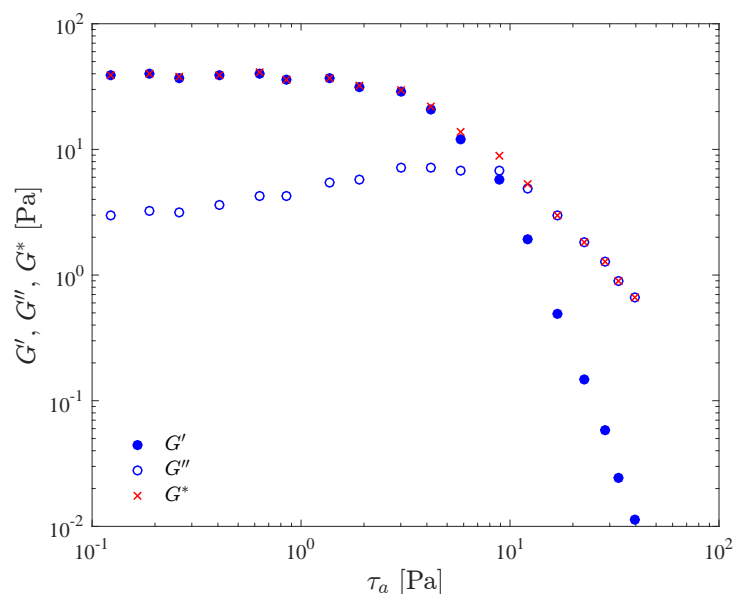
**Figure 1.** Stress amplitude sweep test results for a 0.123 wt% Carbopol aqueous dispersion.

Figure 1 can be divided into three regions, namely the linear viscoelastic region (LVR), the yielding region, and the non-linear region. The LVR occurs in the low stress amplitude range, and is characterized by constant (i.e., stress-amplitude independent) moduli. It corresponds to the so-called "small-amplitude oscillatory shear" (SAOS) flow regime. Both the yielding and the non-linear region are in the domain of the so-called "large-amplitude oscillatory shear" (LAOS) flow regime.

In the LVR, the imposed stress is small in comparison to the strength of the bonds that sustain the microstructure, so that its integrity is unaffected. The microgels remain in their "cages", i.e., are allowed to deform elastically but do not move significantly relative to each other. This microstructure confers a predominantly elastic behavior to the material, as indicated by a large G' in comparison with G''. The elastic preponderance indicates a low internal dissipation within microgels [16].

At this point it is interesting to emphasize that the definitions of G' and G'' originate from the assumption that both the input and output waves be sinusoidal, i.e., that the stress depends linearly on the shear strain and on the shear rate. In other words, G' and G'' cannot depend on the stress amplitude,

by definition. Therefore, in principle the values of G' and G'' shown in Figure 1 would be meaningless beyond the LVR, because they do depend on the stress amplitude. There is no guarantee that the output (strain) wave is sinusoidal outside the LVR, in potential conflict with the basic hypothesis of the theory from which G' and G'' arise. This fact is typically overlooked in the literature, probably because the trends observed for G' and G'' beyond the LVR seem to be in qualitative agreement with the expected behavior.

The reason for the successful performance of G' and G'' outside their domain is the fact that in this case the output waves are not too far from sinusoidal beyond the SAOS regime. This is illustrated in Figure 2. That is, for this Carbopol dispersion at 1 Hz (and seemingly for Carbopol dispersions in general at 1 Hz), the so-called quasilinear large-amplitude oscillatory shear (QL-LAOS) flow regime prevails beyond the LVR. The existence of this regime was recently discovered theoretically by [62] and later confirmed experimentally [63]. The quasilinearity (sinusoidal output wave) occurs because at a given stress amplitude the microscopic state does not change along the cycle (as in SAOS), although it changes with the stress amplitude, in contrast to what is observed in the SAOS regime. The microscopic state remains unchanged along the cycle because the characteristic time needed for changes in the microscopic state is longer than the characteristic time of the flow, namely $1/2\pi$ s in the present case.
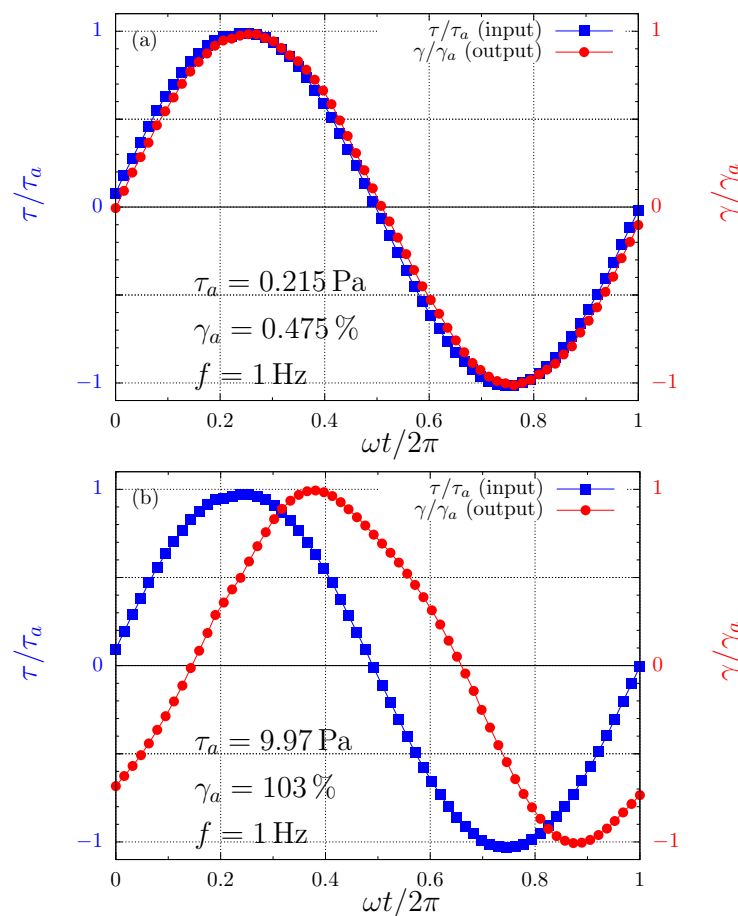
Figure 2. The input and output waves for two different stress amplitudes. (**a**) $\tau_a = 0.215$ Pa [in the linear viscoelastic region (LVR)]; and (**b**) $\tau_a = 9.97$ Pa (in the yielding region).

In addition, the characteristic time needed for changes in the microscopic state is expected to decrease as the stress amplitude is increased, i.e., the microstructure is expected to break faster at larger stresses. Therefore, at large enough stress amplitudes the output waves should cease to be sinusoidal, i.e., the flow

should no longer be within the QL-LAOS regime. This is because, when the time required for changes in the microscopic state is shorter or comparable with the characteristic time of the flow (namely the cycle period), then the microscopic state changes along the cycle. Since the mechanical behavior is a function of the microscopic state, the mechanical behavior varies along the cycle, rendering the output wave non-sinusoidal. In our experiments, however, we did not attain large enough stress amplitudes to leave significantly the QL-LAOS regime.

The dependence of G' and G'' on the stress amplitude is a result of the onset of a bond breaking process (yielding). The larger the stress amplitude the lower the structuring level, which results in less elasticity, as indicated by the decreasing G' as the stress amplitude is increased. In the yielding region, located in the middle range of stress amplitude and around the crossover point, the stress amplitude is high enough to cause some bond breaking, i.e., some microgels escape from their cages and more relative motion occurs. The frictional forces that arise due to relative motion dissipate more mechanical energy, which explains the increase in G''. Within this range of stress amplitude the structuring level is still high enough to retain a percolated microstructure and a sizable elasticity response, as indicated by the still high values of G' found in this region.

It is tempting to take a characteristic stress amplitude of the yielding region as the yield stress, because it is throughout this region that yielding takes place. An obvious choice of characteristic stress amplitude would be the one at which the G' and G'' curves cross. However, the crossover stress amplitude depends to a great extent on the frequency of oscillation, while the definition of yield stress precludes such a dependence. This frequency dependence occurs because the bond breaking process depends both on the stress intensity and on the time period during which the imposed stress persists, in consonance with the discussion above regarding the characteristic time needed for changes in the microscopic state. The larger the imposed stress the lower the time period required to break the bonds, and vice versa. Therefore, in oscillatory flows, for a given stress amplitude the larger the frequency the shorter the stress persistence. Hence, for larger frequencies (shorter stress persistencies) larger stress amplitudes are required to break the bonds. In view of this discussion it might be argued that the yield stress can be identified as the limit as the frequency approaches zero of the crossover stress amplitude. However, as the frequency is reduced, the output wave will eventually cease to be sinusoidal, and hence G' and G'' will lose their physical meanings.

The non-linear region starts beyond the crossover point, where G'' attains its maximum and starts decreasing, and where G' starts decreasing much faster than G''. The high stress amplitudes found in this region cause a massive bond breakage, so that the microstructure is no longer percolated. This confers a liquid behavior to the material. Moreover, the higher the stress amplitude, the lower the structuring level, leading to a more viscous and less elastic behavior.

Figure 3 shows the complex shear modulus as a function of the stress amplitude for three different dispersions, namely two in water and one in a water/glycerol solution. Comparing the results for the two aqueous dispersions, it is seen that G^* is larger for the more concentrated one throughout the stress amplitude range, as expected. Moreover, the LVR range does not change significantly with concentration, as also observed by [38].

Figure 3 also illustrates the influence of the solvent on the complex modulus. It is seen that the G^* curve for the water/glycerol Carbopol dispersion lies below the curves for the two aqueous dispersions, despite the fact that its Carbopol concentration is the highest, illustrating that the presence of glycerol reduces the complex modulus. Since in the LVR $G^* \approx G'$ for the three dispersions, this G^* reduction indicates that glycerol leads to a less elastic structure. The presence of glycerol slightly increases the loss modulus (not shown), as a consequence of the fact that glycerol is more viscous than water. It is interesting to observe that the 0.1 wt% Carbopol aqueous dispersion and the 0.125 wt% Carbopol dispersion in water/glycerol were designed to possess the same yield stress, namely $\tau_y = 2.7$ Pa.
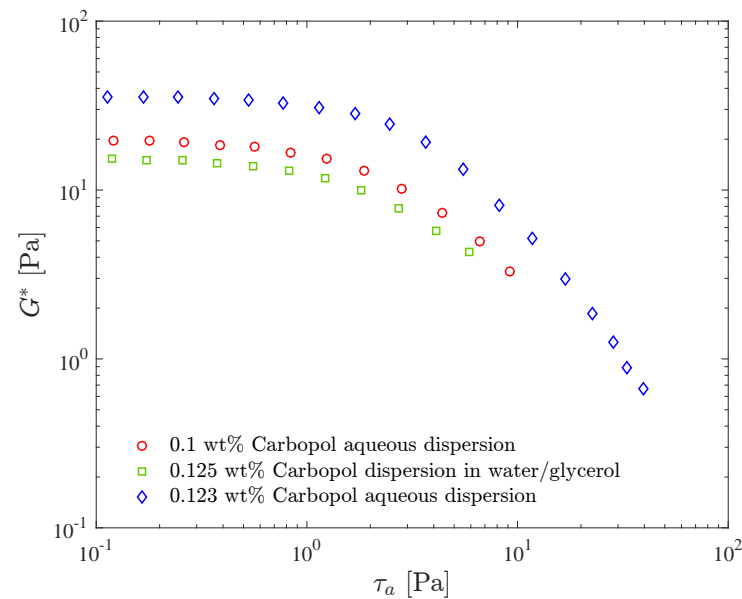
Figure 3. Stress amplitude sweep test resuts for three Carbopol dispersions: effects of the concentration and of the solvent.

3.1.1. Frequency Sweep Tests

Frequency sweep tests are a useful tool to assess the mechanical response of the material microstructure in its quiescent state [23]. It is known that the magnitude of the storage modulus G' can be related to the molecular weight and network density [18]. In this test, the stress amplitude is kept constant at a value low enough to ensure that the flow is kept within the linear viscoelastic regime throughout the range of frequency.

Figure 4 shows the storage modulus G' and the loss modulus G'' as a function of the frequency, for the 0.1 wt% aqueous Carbopol dispersion and for the 0.125 wt% Carbopol dispersion in the water/glicerol solution. It is worth recalling that the composition of these two solutions were chosen such that both possess the same yield stress. Comparison of the curves for the two dispersions illustrates the influence of the solvent type on the moduli.

It is seen in this figure that our data lie within the classic rubbery region (or frequency range) [54], since G' remains essentially constant and much larger than G'' throughout the frequency range, as expected for viscoelastic solids and crosslinked systems [64,65]. The G'' curves, on the other hand, increase with frequency.

Moreover, it is seen in this figure that the G' and G'' curves for the two materials are essentially coincident, except towards the high end of the frequency range, where the curve for G'' the aqueous dispersion lies below the one for the dispersion in water/glycerol, while for the G' curves the reverse is true. This indicates that more mechanical energy is dissipated at larger frequencies, and that the more viscous continuous phase tends to dissipate more energy. Moreover, the fact that the moduli of the two dispersions are essentially coincident suggests that the yield stress and the moduli—which are completely distinct properties—are closely related to the microstructure characteristics at its quiescent state, which is expected to be similar for both dispersions.
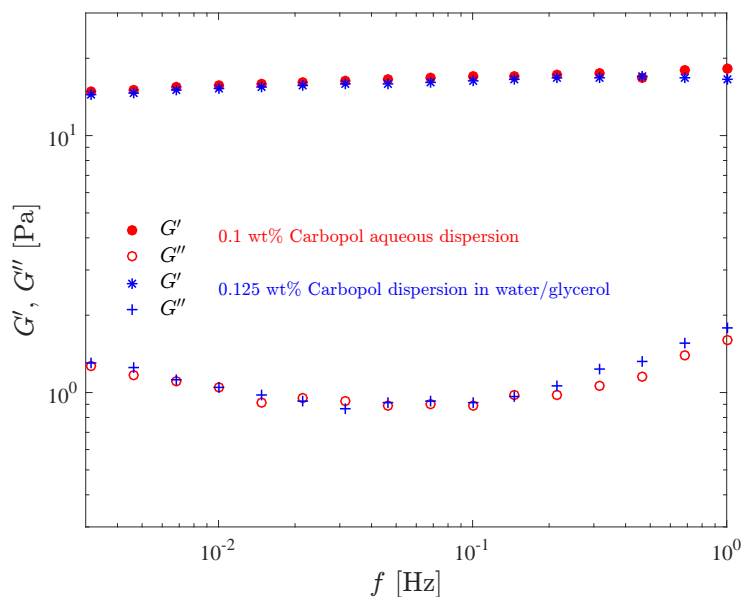
Figure 4. Results of the frequency sweep test for the Carbopol dispersions with the same yield stress.

3.1.2. Time Sweep Tests

The time sweep test consists of observing how the moduli change over time for a constant frequency and stress amplitude. The choice of stress amplitude and frequency should be such as to ensure that the flow is within the linear viscoelastic regime, i.e., the imposed stresses should be negligible when compared to the strength of the microstructure. This test is usually employed to investigate the material stability, i.e., if microscopic changes occur over time. Useful information such as polymer degradation, molecular weight building, cross-linking, solvent evaporation, sedimentation, setting and curing can be obtained with this test. It also allows the determination of the maximum time duration of a test to ensure that none of the just listed effects will interfere in the results.

Figure 5 compares the complex modulus G^* time sweep results for the 0.1 wt% Carbopol aqueous dispersion and for the 0.125 wt% dispersion of Carbopol in water/glycerol solution. Both curves were obtained at 1 Hz and at stress amplitudes well below the yield stress (which is 2.7 Pa), namely 0.08 and 0.1 Pa, respectively.

The results in Figure 5 show that the dispersions under investigation are very stable and free from aging, as indicated by the fact that the G^* curves are essentially horizontal, except for a very short transient behavior probably due to microstructure rebuilding after sample loading. The curve for the water/glycerol dispersion lies above the one for the aqueous dispersion, in accordance with the discussion and results presented above.
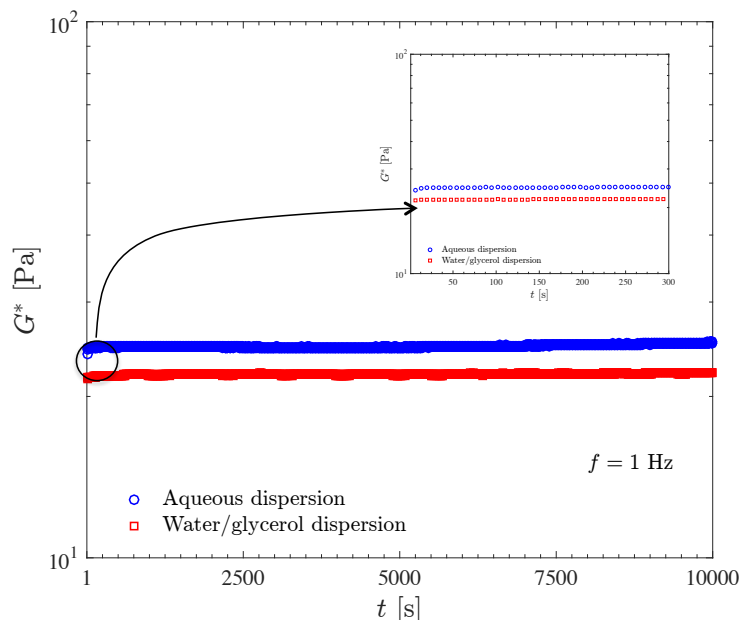
Figure 5. Evaluation of the stability of Carbopol dispersions by means of the time sweep test.

3.2. Constant Shear Rate Tests

Figure 6 shows the transient viscosity of the two Carbopol dispersions that possess the same yield stress. In this test, the sample is loaded on the rheometer and left to rest for a few minutes to allow for the microstructure reconstruction. Then, at time $t = 0$ we impose a constant shear rate, and record the transient shear stress (or viscosity) response. Due to the error caused by the instrument inertia, the data pertaining to the first second of each test were discarded.
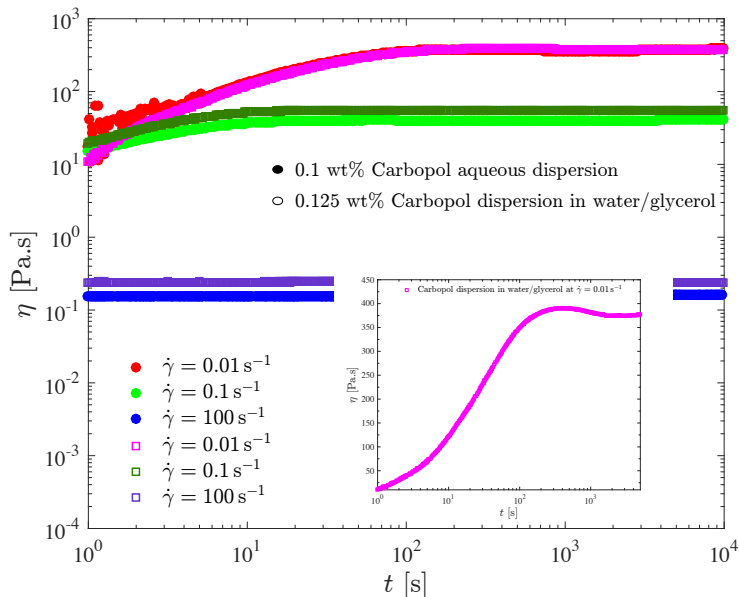

Figure 6. The constant shear rate test for the dispersions with the same yield stress.

For both dispersions and all shear rate values investigated, it is seen in Figure 6 that the viscosity eventually reaches a steady state. The larger the shear rate the lower the steady-state viscosity, because

larger shear rates imply larger shear stresses, which in turn result in more intense microstructure breakdown. Consequently, structuring levels pertaining to larger shear rates are lower, and there is a one-to-one relationship between the steady-state viscosity and the structuring level (e.g., [62,66,67]).

Figure 6 also shows that for both dispersions the time required for the steady state to be reached, say t_{ss}, decreases as the shear rate is increased. Specifically, $t_{ss} \approx 100; 10; 0\,\mathrm{s}$ for $\dot{\gamma} = 0.01; 0.1; 100\,\mathrm{s}^{-1}$, respectively. These results are in agreement with the generally accepted rule of thumb $t_{ss} \approx 1/\dot{\gamma}$ used to estimate t_{ss}. To understand this trend we first note that the steady-state stresses corresponding to very low shear rates are always very close to the yield stress, while for high shear rates the corresponding shear stresses are well above the yield stress. Therefore, the long times required for the achievement of the steady state at low shear rates mean that the Carbopol dispersions display a sizable thixotropic effect when the stress is very close but above the yield stress. For larger stresses there is no thixotropy, as indicated by the very short times required for the steady state to be achieved.

The shear stress evolution with time is well illustrated by the curve for the 0.125 wt% Carbopol dispersion in glycerol/water at $\dot{\gamma} = 0.01\,\mathrm{s}^{-1}$, highlighted in the insert of Figure 6. At time $t < 0$, the gel is unstrained and fully structured, and thus it is a viscoelastic solid. At $t = 0$, when the shear rate jump occurs, a corresponding shear stress jump is expected due to an initially purely viscous response of the still unstrained sample. This viscous contribution to the stress is expected to remain fixed while the material remains fully structured, because the shear rate remains fixed in this test. The strain increases linearly, starting from zero at $t = 0$, causing the growth (also from zero) of the elastic contribution to the stress.

At large enough strains (but still below the yield point), the elastic contribution to the stress becomes much larger than the viscous one, and a linear growth of the (total) stress is observed. When the stress reaches the yield stress, the microstructure undergoes a major collapse and ceases to be percolated, and hence the material becomes a viscoelastic liquid and eventually a steady state is reached.

A sizable stress overshoot followed by a slight undershoot is observed in this curve, because in this case the imposed shear rate is small enough to cause stresses just above the yield stress, so that the microstructure does not respond instantaneously to the stress changes (i.e., thixotropic behavior).

For larger imposed shear rate values, most of the features of the stress evolution described here for $\dot{\gamma} = 0.01\,\mathrm{s}^{-1}$ are expected to be preserved, but occur too fast to be observable in this test.

The influence of the solvent type on the transient viscosity is quite mild. It is observed that for the lower shear rates, slightly longer t_{ss} values are required for Carbopol dispersions in water/glycerol. This suggests that the breakup process is hindered by the higher viscosity of the water/glycerol solution.

3.3. Flow Curves

The effect of the type of solvent and Carbopol concentration on the flow curve is illustrated in Figure 7, where the (steady-state) shear stress is given as a function of the shear rate for the 0.1 wt%, 0.123 wt% and the 0.125 wt% Carbopol aqueous dispersions, and also for the 0.125 wt% and 0.15 wt% Carbopol dispersions in the water/glycerol solution.

All flow curves are obtained by decreasing the shear rate from 100 to $10^{-3}\,1/\mathrm{s}$. This procedure reduces significantly the time duration of the tests, as compared to imposing ascending shear rate values. It is worth emphasizing the importance of determining a large enough time $t \geq t_{ss}$ at each applied shear rate, to allow steady state to be achieved before moving to the next shear rate value. As mentioned above, the steady-state time can be estimated as $t_{ss} \approx 1/\dot{\gamma}$. In our experiments, we impose each shear rate value for a maximum period of 1000 s. At each 30 s, an averaged torque is recorded. After three consecutive 30-s periods the corresponding values of the averaged torque are compared, and steady state is assumed when they are the same within 0.1%.
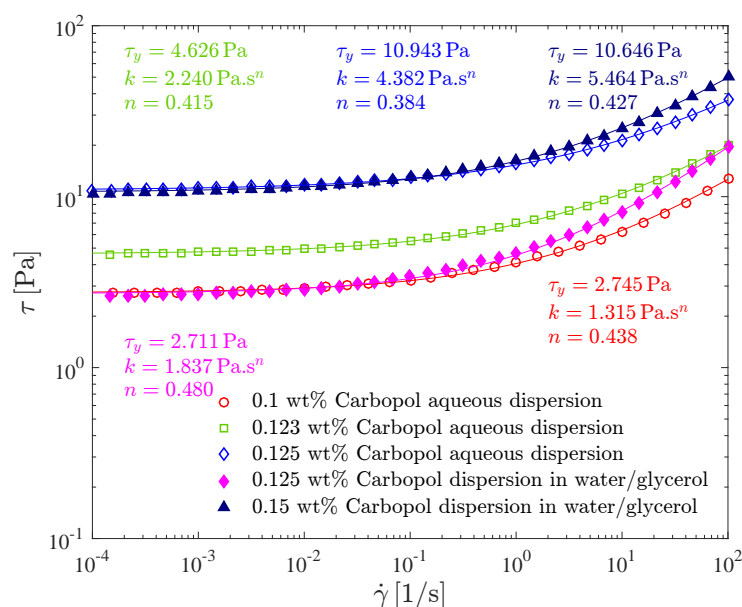
Figure 7. Solvent and polymer concentration influence on flow curve tests: shear stress as a function of shear rate.

The range of shear rate is limited from below by the rheometer torque resolution and from above by sample inertia effects. In addition, the use of cross-hatched parallel plates should be limited to moderate shear stresses, to avoid the occurrence of flow within the protuberances. In this connection, a smooth Couette geometry was used in the range between 3000 and $100 \, \mathrm{s}^{-1}$.

All the flow curves given in Figure 7 possess the usual Herschel-Bulkley shape. In addition, all of them are monotonic, indicating that shear banding does not occur [68,69].

The Herschel-Bulkley parameters for all curves are also given in Figure 7. As expected, it is seen that, for a given continuous phase, increasing the Carbopol concentration causes both the yield stress and the consistency index to increase, and the power law index to slightly decrease [70]. Moreover, the values found for the power-law index ranged from 0.38 to 0.48, in good agreement with the observations of [17].

It can be seen in Figure 7 that the flow curve for the 0.125 wt% aqueous dispersion lies well above the one for the 0.125 wt% dispersion in water/glycerol, demonstrating that at the same, Carbopol concentration, the one with a more viscous solvent, possesses a significantly lower viscosity level. In addition, the dispersion in water/glycerol possesses a higher power-law index than the aqueous dispersion, and hence the former is less pseudoplastic than the latter.

Comparing now the flow curves of two dispersions with the same yield stress (0.1 wt% aqueous dispersion and 0.125 wt% dispersion in water/glycerol; and 0.125 wt% aqueous dispersion and 0.15 wt% dispersion in water/glycerol), the dispersions in water/glycerol possess a viscosity level higher than the one of the corresponding aqueous dispersions, as it can be directly observed in Figure 7.

3.4. Creep Tests

The creep test consists of imposing a constant shear stress to an initially unstrained and fully structured sample, and recording the time evolution of the shear rate (or viscosity). It is commonly employed to assess viscoplastic and thixotropic effects of complex fluids, and especially to measure the yield stress [9,71–73]. A number of creep tests are required in order to identify the yield stress: if the imposed stress is lower than the yield stress, then the shear rate approaches zero as a maximum elastic strain is approached, as expected

for solids of amorphous microstructure [60,61,74]; and if the imposed stress is above the yield stress then the shear rate eventually attains a constant (steady-state) value [75].

The yield stress obtained from creep tests is the so-called static yield stress, $\tau_{y,s}$, i.e., it is the stress needed to cause irreversible flow on a sample initially unstrained and fully structured [9,71,72]. In contrast, the shear stress obtained from curve fitting to data of a flow curve test is the so-called dynamic yield stress, $\tau_{y,d}$. In general, these two yield stresses are distinct from each other, the dynamic yield stress being smaller than static yield stress [71].

Figure 8 presents creep test results for the 0.1 wt% Carbopol aqueous dispersion and for the 0.125 wt% Carbopol dispersion in water/glycerol. In Figure 8a the shear rate is plotted as a function of time, while in Figure 8b the same data are plotted as a function of the shear strain, $\gamma = \int_0^t \dot{\gamma} dt'$. For all curves shown in Figure 8, the data obtained below one second were discarded due to contamination with the instrument inertia [76,77]. Therefore, for each curve in Figure 8b a different initial strain is observed.

Figure 8 illustrates that the two dispersions possess similar static yield stresses, namely between 4 and 5 Pa for the dispersion in water/glycerol and between 3.5 and 4 Pa for the aqueous dispersion. It is noted that the curve for 4 Pa pertaining to the aqueous dispersion possesses a minimum at about 1400 s (or at a Hencky strain of about 2.5). Therefore, at 4 Pa the sample deformed elastically up to about 1400 s and then the microstructure collapsed, leading to the onset of irreversible flow. This long time delay before the occurrence of yielding is usually referred to as the avalanche effect [78], and is another manifestation of the thixotropic behavior of Carbopol dispersions when the imposed stress is very close but above the yield stress. It is interesting to comment that had we conducted the creep tests for 1000 s only, we would have concluded that the static yield stress of the aqueous dispersion is above 4 Pa, because at this point there was no sign of irreversible flow. On the other hand, if the tests had lasted for two hours, for example, it is possible that the aqueous dispersion would flow at stresses below 3.5 Pa. Therefore, the static yield stress obtained with this test is a function of the time duration of the test. In fact, this is also true for any other method for measuring the yield stress, as extensively discussed in the literature (e.g., [62]).

Ref. [36] observed a similar behavior for a dispersion of Carbopol ETD 2050, and interpreted it as an avalanche-like behavior involving wall slip and transient shear banding. They assumed the Carbopol dispersion as a "simple yield stress fluid", i.e., a non-thixotropic viscoplastic material. A roughened Couette cell was employed and shear-rate controlled experiments were performed. The same behavior was later reported by [79] for shear-stress controlled experiments. On the other hand, the transient shear banding phenomenon was not observed by [80] under similar conditions for a yield stress fluid. Ref. [81] affirm that steady state is very difficult to be achieved under the influence of wall slip. Likewise, they observed that the solid-liquid transition is not reversible upon increasing or decreasing of the applied stresses, due to elastic and thixotropic effects. According to [82], imposing a constant shear stress, the glass fluidization near yielding is very slow, and persistent spatial heterogeneities remain present. Ref. [83] obtained a monotonic flow curve for a material that presented a time delay before yielding [78], and concluded that thixotropy cannot be ignored. More recently, Ref. [84] emphasized that the preparation procedure of Carbopol dispersions is of paramount importance as far as the final mechanical behavior is concerned. Low stirring times lead to large (non-colloidal) microgels and a non-thixotropic behavior. Long stirring times, on the other hand, lead to colloidal microgels and a time-dependent behavior. All this discussion attests that the physical origin of the time delay before yielding is not fully understood.
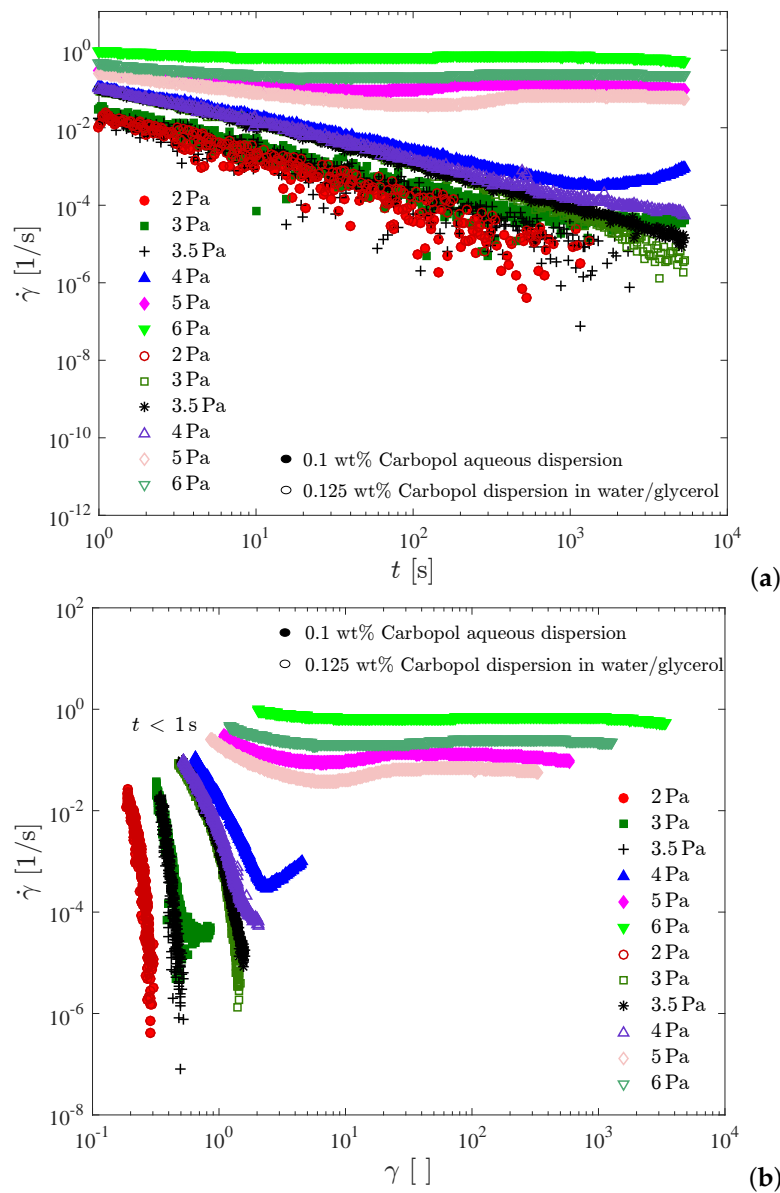
Figure 8. The creep tests. (**a**) Shear rate *vs.* time; (**b**) Shear rate *vs.* strain.

3.5. Constant Shear Rate vs. Constant Shear Stress Tests

Figure 9 presents a comparison between results obtained by imposing a constant shear rate, as in Figure 6, and a constant shear stress, as in Figure 8. For each dispersion, the values of imposed stress and shear rate were selected such that the steady-state viscosity was roughly the same both for imposed stress and rate.

For both dispersions considered in Figure 9, a viscosity overshoot is observed when a constant shear stress just above the yield stress is applied. On the other hand, imposing a constant shear rate leads to a much milder and difficult to observe viscosity overshoot, and to a faster achievement of steady state.
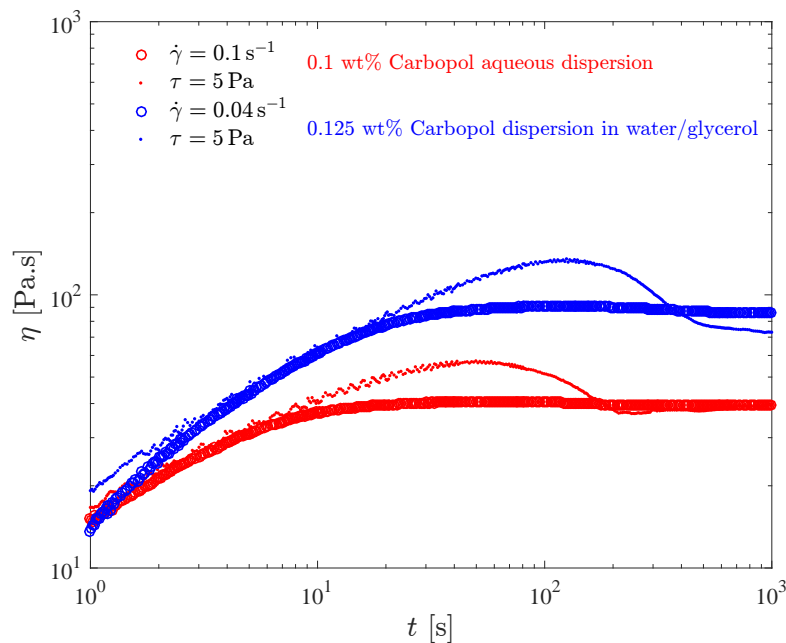
Figure 9. The transient viscosity obtained in constant-stress and constant-rate tests.

This behavior can be explained by observing that the viscosity overshoot that occurs with the application of a constant stress just above the yield stress is due to thixotropy, i.e., due to the time lag that is observed between the application of the stress and the microstructure collapse (yielding). Moreover, the viscosity overshoot is milder when the shear rate is imposed because in this case the transient shear stress is larger, which reduces or eliminates the thixotropic effect.

Creep-Recovery Tests

The creep-recovery test consists of imposing a stress above the yield stress until steady state is achieved, and then imposing a step change to a stress below the yield stress. The shear strain is recorded, and plotted as a function of time. This test is useful to assess the elasticity of the yielded material and also to provide the time required for the microstructure to rebuild. During the first step of the test, namely when a stress above the yield stress is imposed, the structuring level is brought down to a certain extent, while during the second step when the stress is below the yield stress the microstructure rebuilds.

Figure 10 presents the time evolution of the shear strain for the 0.1 wt% Carbopol aqueous dispersion and the 0.125 wt% Carbopol dispersion in water/glycerol. Upon inspection of these figures, it becomes clear that the qualitative behavior of both solutions is the same. The results indicate that the dispersions possess no elasticity whatsoever at the structuring levels that correspond to 5 and 3.5 Pa respectively, as attested by the absence of recoil right after the stress reduction. Another result is that the microstructure of both dispersions rebuild instantaneously, since no flow is observed after the stress reduction.
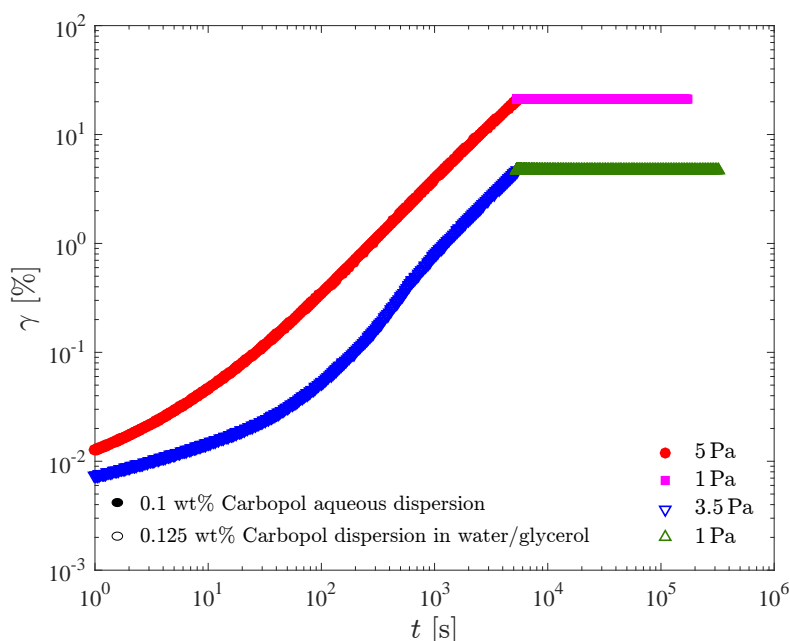
Figure 10. The strain evolution in the creep-recovery test for two Carbopol dispersions.

4. Final Remarks

The rheological properties of Carbopol dispersions in water and in water/glycerol solutions were investigated for concentrations ranging from 0.1 to 0.15 wt%. The preparation procedure and rheological experiments were discussed in detail.

For both formulations, an elasto-viscoplastic behavior was observed as well as a remarkable material stability over time (no aging). The elastic effects are dominant when the microstructure is fully structured, while viscous effects dominate after yielding. At stresses just above the yield stress, thixotropic effects are observed, in contrast to the observed absence of thixotropy at larger stresses. No elasticity was observed in the dispersions while unstructured, and their microstructure rebuilds instantaneously after reduction of the imposed stress to a value below the yield stress.

Comparing aqueous dispersions with dispersions in water/glycerol for the same Carbopol concentration, it is shown that the dispersion in water/glycerol possesses lower yield stress and moduli, while the power-law index is larger (less shear thinning) and the time required for steady state is longer.

Conflicts of Interest: The authors declare no conflict of interest.

References

1. Barnes, H.A.; Walters, K. The yield stress myth? *Rheol. Acta* **1985**, *24*, 323–326. [CrossRef]
2. Barnes, H.A. The yield stress—A review or 'panta rei'—Everything flows? *J. Non-Newton. Fluid Mech.* **1999**, *81*, 133–178. [CrossRef]
3. Astarita, G. The Engineering Reality of The Yield Stress. *J. Rheol.* **1990**, *34*, 275–277. [CrossRef]
4. Hartnett, J.P.; Hu, R.Y.Z. The yield stress—An engineering reality. *J. Rheol.* **1989**, *33*, 671–679. [CrossRef]
5. Evans, I.D. On the nature of the yield stress. *J. Rheol.* **1992**, *36*, 1313–1316. [CrossRef]
6. Nguyen, Q.D.; Boger, D.V. Measuring the flow properties of yield stress fluids. *Annu. Rev. Fluid Mech.* **1992**, *24*, 47–88. [CrossRef]
7. Møller, P.C.F.; Mewis, J.; Bonn, D. Yield stress and thixotropy: On the difficulty of measuring yield stresses in practice. *Soft Matter* **2006**, *2*, 274–283. [CrossRef]
8. Moller, P.; Fall, A.; Bonn, D. Origin of apparent viscosity in yield stress fluids below yielding. *EPL (Europhys. Lett.)* **2009**, *87*, 38004. [CrossRef]
9. Balmforth, N.J.; Frigaard, I.A.; Ovarlez, G. Yielding to Stress: Recent Developments in Viscoplastic Fluid Mechanics. *Annu. Rev. Fluid Mech.* **2014**, *46*, 121–146. [CrossRef]
10. Carnali, J.O.; Naser, M.S. The use of dilute solution viscometry to characterize the network properties of carbopol microgels. *Colloid Polym. Sci.* **1992**, *270*, 183–193. [CrossRef]
11. Magnin, A.; Piau, J. Cone-and-plate rheometry of yield stress fluids. Study of an aqueous gel. *J. Non-Newton. Fluid Mech.* **1990**, *36*, 85–108. [CrossRef]
12. Alba, K.; Taghavi, S.M.; Bruyn, J.R.; Frigaard, I. Incomplete fluid–fluid displacement of yield-stress fluids. Part 2: Highly inclined pipes. *J. Non-Newton. Fluid Mech.* **2013**, *201*, 80–93. [CrossRef]
13. Coussot, P. Yield stress fluid flows: A review of experimental data. *J. Non-Newton. Fluid Mech.* **2014**, *211*, 31–49. [CrossRef]
14. Jørgensen, L.; Le Merrer, M.; Delanoë-Ayari, H.; Barentin, C. Yield stress and elasticity influence on surface tension measurements. *Soft Matter* **2015**, *11*, 5111–5121. [CrossRef] [PubMed]
15. Roberts, G.P.; Barnes, H.A. New measurements of the flow-curves for Carbopol dispersions without slip artefacts. *Rheol. Acta* **2001**, *40*, 499–503. [CrossRef]
16. Piau, J.M. Carbopolgels: Elastoviscoplastic and slippery glasses made of individual swollen sponges. Meso- and macroscopic properties, constitutive equations and scaling laws. *J. Non-Newton. Fluid Mech.* **2007**, *144*, 1–29. [CrossRef]
17. Gutowski, I.A.; Lee, D.; de Bruyn, J.R. Scaling and mesostructure of Carbopol dispersions. *Rheol. Acta* **2012**, *51*, 441–450. [CrossRef]
18. Ahmed, E.M. Hydrogel: Preparation, characterization, and applications: A review. *J. Adv. Res.* **2015**, *6*, 105–121. [CrossRef]
19. Taylor, N.W.; Bagley, E.B. Dispersions or Solutions? A Mechanism for Certain Thickening Agents. *J. Appl. Polym. Sci.* **1974**, *18*, 2747–2761. [CrossRef]
20. Putz, A.; Burghelea, T. The solid-fluid transition in a yield stress shear thinning physical gel. *Rheol. Acta* **2009**, *48*, 673–689. [CrossRef]
21. Brodnyan, J.G.; Kelley, E.L. The Rheology of Polyelectrolytes. I. Flow Curves of Concentrated Poly(acrylic Acid) Solutions. *Trans. Soc. Rheol.* **1961**, *5*, 205–220. [CrossRef]
22. Fischer, W.H.; Bauer, W.H.; Wiberley, S.E. Yield Stresses and Flow Properties of Carboxypolymethylene Water Systems. *Trans. Soc. Rheol.* **1961**, *5*, 221–235. [CrossRef]
23. Kim, J.Y.; Song, J.Y.; Lee, E.J.; Park, S.K. Rheological properties and microstructures of Carbopol gel network system. *Colloid Polym. Sci.* **2003**, *281*, 614–623. [CrossRef]
24. Bonn, D.; Denn, M.M.; Berthier, L.; Divoux, T.; Manneville, S. Yield stress materials in soft condensed matter. *Rev. Mod. Phys.* **2017**, *89*, 035005. [CrossRef]
25. Larson, R.G. *The Structure and Rheology of Complex Fluids*; Oxford University Press Inc.: New York, NY, USA, 1999.

26.　Oppong, F.K.; Rubatat, L.; Frisken, B.J.; Bailey, A.E.; de Bruyn, J.R. Microrheology and structure of a yield-stress polymer gel. *Phys. Rev. E* **2006**, *73*, 041405. [CrossRef] [PubMed]

27.　Yoshimura, A.S.; Prud'homme, R.K. Response of an elastic Bingham fluid to oscillatory shear. *Rheol. Acta* **1987**, *26*, 428–436. [CrossRef]

28.　Al-Hadithi, T.S.R.; Barnes, H.A.; Walters, K. The relationship between the linear (oscillatory) and nonlinear (steady-state) flow properties of a series of polymer and colloidal systems. *Colloid Polym. Sci.* **1992**, *270*, 40–46. [CrossRef]

29.　Barry, B.; Meyer, M. The rheological properties of Carbopol gels I. Continuous shear and creep properties of Carbopol gels. *Int. J. Pharm.* **1979**, *2*, 1–25. [CrossRef]

30.　Islam, M.T.; Rodríguez-Hornedo, N.; Ciotti, S.; Ackermann, C. Rheological Characterization of Topical Carbomer Gels Neutralized to Different pH. *Pharm. Res.* **2004**, *21*, 1192–1199. [CrossRef]

31.　Di Giuseppe, E.; Corbi, F.; Funiciello, F.; Massmeyer, A.; Santimano, T.N.; Rosenau, M.; Davaille, A. Characterization of Carbopol hydrogel rheology for experimental tectonics and geodynamics. *Tectonophysics* **2015**, *642*, 29–45. [CrossRef]

32.　Moller, P.; Fall, A.; Chikkadi, V.; Derks, D.; Bonn, D. An attempt to categorize yield stress fluid behaviour. *Philos. Trans. R. Soc. Lond. A Math. Phys. Eng. Sci.* **2009**, *367*, 5139–5155. [CrossRef] [PubMed]

33.　Coussot, P.; Tocquer, L.; Lanos, C.; Ovarlez, G. Macroscopic vs. local rheology of yield stress fluids. *J. Non-Newton. Fluid Mech.* **2009**, *158*, 85–90. [CrossRef]

34.　Herschel, V.W.H.; Bulkley, R. Konsistenzmessungen von Gummi-Benzollösungen. *Colloid Polym. Sci.* **1926**, *39*, 291–300. [CrossRef]

35.　Tabuteau, H.; Coussot, P.; de Bruyn, J.R. Drag force on a sphere in steady motion through a yieldstress fluid. *J. Rheol.* **2007**, *51*, 125–137. [CrossRef]

36.　Divoux, T.; Tamarii, D.; Barentin, C.; Manneville, S. Transient Shear Banding in a Simple Yield Stress Fluid. *Phys. Rev. Lett.* **2010**, *104*, 208301. [CrossRef] [PubMed]

37.　Weber, E.; Moyers-González, M.; Burghelea, T.I. Thermorheological properties of a Carbopol gel under shear. *J. Non-Newton. Fluid Mech.* **2012**, *183–184*, 14–24. [CrossRef]

38.　Ketz, R.J.; Prud'homme, R.K.; Graessley, W.W. Rheology of concentrated microgel solutions. *Rheol. Acta* **1988**, *27*, 531–539. [CrossRef]

39.　Nelson, A.Z.; Ewoldt, R.H. Design of yield-stress fluids: A rheology-to-structure inverse problem. *Soft Matter* **2017**, *13*, 7578–7594. [CrossRef]

40.　Nelson, A.Z.; Bras, R.E.; Liu, J.; Ewoldt, R.H. Extending yield-stress fluid paradigms. *J. Rheol.* **2018**, *62*, 357–369. [CrossRef]

41.　Chu, J.S.; Yu, D.M.; Amidon, G.L.; Weiner, N.D.; Goldberg, A.H. Viscoelastic Properties of Polyacrylic Acid Gels in Mixed Solvents. *Pharm. Res.* **1992**, *9*, 1659–1663. [CrossRef]

42.　Proniuk, S.; Blanchard, J. Anhydrous Carbopol polymer gels for the topical delivery of oxygen/water sensitive compounds. *Pharm. Dev Technol.* **2002**, *7*, 249–255. [CrossRef] [PubMed]

43.　Corporation, T.L. *Neutralizing Carbopol and Pemulen Polymers in Aqueous and Hydroalcoholic Systems*; Technical Report TDS-237; The Lubrizol Corporation: Wickliffe, OH, USA, 2009.

44.　Bonacucina, G.; Cespi, M.; Misici-Falzi, M.; Palmieri, G.F. Rheological evaluation of silicon/carbopol hydrophilic gel systems as a vehicle for delivery of water insoluble drugs. *AAPS J.* **2008**, *10*, 84–91. [CrossRef] [PubMed]

45.　Noveon, I. *Formulating Topical Properties*; Technical Report Bulletin 14; Noveon Inc.: Cleveland, OH, USA, 2002.

46.　Corporation, T.L. *Molecular Weight of Carbopol and Pemulen Polymers*; Technical Report TDS-222; The Lubrizol Corporation: Wickliffe, OH, USA, 2007.

47.　Corporation, T.L. *Dispersion Techniques for Carbopol Polymers*; Technical Report TDS-103; The Lubrizol Corporation: Wickliffe, OH, USA, 2007.

48.　Corporation, T.L. *Formulating Hydroalcoholic Gels with Carbopol Polymers*; Technical Report TDS-255; The Lubrizol Corporation: Wickliffe, OH, USA, 2009.

49.　Sikorski, D.; Tabuteau, H.; de Bruyn, J. Motion and shape of bubbles rising through a yield-stress fluid. *J. Non-Newton. Fluid Mech.* **2009**, *159*, 10–16. [CrossRef]

50. Krieger, I.M. Bingham Award Lecture—1989: The role of instrument inertia in controlled-stress rheometers. *J. Rheol.* **1990**, *34*, 471–483. [CrossRef]

51. Baravian, C.; Quemada, D. Using instrumental inertia in controlled stress rheometry. *Rheol. Acta* **1998**, *37*, 223–233. [CrossRef]

52. Baravian, C.; Benbelkacem, G.; Caton, F. Unsteady rheometry: Can we characterize weak gels with a controlled stress rheometer? *Rheol. Acta* **2007**, *46*, 577–581. [CrossRef]

53. Läuger, J.; Stettin, H. Effects of instrument and fluid inertia in oscillatory shear in rotational rheometers. *J. Rheol.* **2016**, *60*, 393–406. [CrossRef]

54. Barnes, H.A. *A Handbook of Elementary Rheology*; University of Wales, Institute of Non-Newtonian Fluid Mechanics: Wales, UK, 2000.

55. Buscall, R.; McGowan, J.I.; Morton-Jones, A.J. The rheology of concentrated dispersions of weakly attracting colloidal particles with and without wall slip. *J. Rheol.* **1993**, *37*, 621–641. [CrossRef]

56. Barnes, H.A. A review of the slip (wall depletion) of polymer solutions, emulsions and particle suspensions in viscometers: Its cause, character, and cure. *J. Non-Newton. Fluid Mech.* **1995**, *56*, 221–251. [CrossRef]

57. Barnes, H.A. Measuring the viscosity of large-particle (and flocculated) suspensions—A note on the necessary gap size of rotational viscometers. *J. Non-Newton. Fluid Mech.* **2000**, *94*, 213–217. [CrossRef]

58. Rabinowitsch, B. Über die Viskosität und Elastizität von Solen. *Z. Phys. Chem.* **1929**, *A145*, 1–26. [CrossRef]

59. De Souza Mendes, P.R.; Alicke, A.A.; Thompson, R.L. Parallel-plate geometry correction for transient rheometric experiments. *Appl. Rheol.* **2014**, *24*, 52721.

60. Lidon, P.; Villa, L.; Manneville, S. Power-law creep and residual stresses in a carbopol gel. *Rheol. Acta* **2017**, *56*, 307–323. [CrossRef]

61. Dimitriou, C.J.; Ewoldt, R.H.; McKinley, G.H. Describing and prescribing the constitutive response of yield stress fluids using large amplitude oscillatory shear stress (LAOStress). *J. Rheol.* **2013**, *57*, 27–70. [CrossRef]

62. De Souza Mendes, P.R.; Thompson, R.L. A unified approach to model elasto-viscoplastic thixotropic yield-stress materials and apparent-yield-stress fluids. *Rheol. Acta* **2013**, *52*, 673–694. [CrossRef]

63. De Souza Mendes, P.R.; Thompson, R.L.; Alicke, A.A.; Leite, R.T. The quasilinear large-amplitude viscoelastic regime and its significance in the rheological characterization of soft matter. *J. Rheol.* **2014**, *58*, 537–561. [CrossRef]

64. Raghavan, S.R.; Chen, L.A.; McDowell, C.; Khan, S.A.; Hwang, R.; White, S. Rheological study of crosslinking and gelation in chlorobutyl elastomer systems. *Polymer* **1996**, *37*, 5869–5875. [CrossRef]

65. Kocen, R.; Gasik, M.; Novak, S. Viscoelastic behaviour of hydrogel-based composites for tissue engineering under mechanical load. *Biomed. Mater.* **2017**, *12*, 025004. [CrossRef]

66. De Souza Mendes, P.R. Modeling the thixotropic behavior of structured fluids. *J. Non-Newton. Fluid Mech.* **2009**, *164*, 66–75. [CrossRef]

67. de Souza Mendes, P.R. Thixotropic elasto-viscoplastic model for structured fluids. *Soft Matter* **2011**, *7*, 2471–2483. [CrossRef]

68. Quemada, D.; Berli, C. Describing the Flow Curve of Shear-Banding Fluids Through a Structural Minimal Model. *arXiv* **2009**, arXiv:0903.0808.

69. Jain, A.; Singh, R.; Kushwaha, L.; Shankar, V.; Joshi, Y.M. Transient start-up dynamics and shear banding in aging soft glassy materials: Rate-controlled flow field. *arXiv* **2018**, arXiv:1801.07088.

70. Hassan, M.A.; Pathak, M.; Khan, M.K. Thermorheological Characterization of Elastoviscoplastic Carbopol Ultrez 20 Gel. *J. Eng. Mater. Technol.* **2015**, *137*, 031002. [CrossRef]

71. Cheng, D.C.H. Yield stress: A time-dependent property and how to measure it. *Rheol. Acta* **1985**, *25*, 542–554. [CrossRef]

72. Mujumdar, A.; Beris, A.N.; Metzner, A.B. Transient phenomena in thixotropic systems. *J. Non-Newton. Fluid Mech.* **2002**, *102*, 157–178. [CrossRef]

73. de Souza Mendes, P.R.; Thompson, R.L. A critical overview of elasto-viscoplastic thixotropic modeling. *J. Non-Newton. Fluid Mech.* **2012**, *187-188*, 8–15. [CrossRef]

74. Da C. Andrade, E.N. On the viscous flow in metals, and allied phenomena. *Proc. R. Soc. Lond. A Math. Phys. Eng. Sci.* **1910**, *84*, 1–12. [CrossRef]

75. Coussot, P.; Nguyen, Q.D.; Huynh, H.T.; Bonn, D. Viscosity bifurcation in thixotropic, yielding fluids. *J. Rheol.* **2002**, *46*, 573–589. [CrossRef]

76. Ferry, J.D. *Viscoelastic Properties of Polymers*; Wiley: New York, NY, USA, 1980.

77. Ewoldt, R.H.; McKinley, G.H. Creep ringing in rheometry or how to deal with oft-discarded data in step stress tests! *Rheol. Bull.* **2007**, *76*, 22–24.

78. Coussot, P.; Nguyen, Q.; Huynh, H.; Bonn, D. Avalanche Behavior in Yield Stress Fluids. *Phys. Rev. Lett.* **2002**, *88*, 175501. [CrossRef]

79. Divoux, T.; Barentin, C.; Manneville, S. From stress-induced fluidization processes to Herschel-Bulkley behaviour in simple yield stress fluids. *Soft Matter* **2011**, *7*, 8409–8418. [CrossRef]

80. Vasu, K.S.; Krishnaswamy, R.; Sampath, S.; Sood, A.K. Yield stress, thixotropy and shear banding in a dilute aqueous suspension of few layer graphene oxide platelets. *Soft Matter* **2013**, *9*, 5874–5882. [CrossRef]

81. Poumaere, A.; Moyers-González, M.; Castelain, C.; Burghelea, T. Unsteady laminar flows of a Carbopol$^{®}$ gel in the presence of wall slip. *J. Non-Newton. Fluid Mech.* **2014**, *205*, 28–40. [CrossRef]

82. Chaudhuri, P.; Horbach, J. Onset of flow in a confined colloidal glass under an imposed shear stress. *Phys. Rev. E* **2013**, *88*, 040301. [CrossRef] [PubMed]

83. Cheng, P.; Burroughs, M.C.; Leal, L.G.; Helgeson, M.E. Distinguishing shear banding from shear thinning in flows with a shear stress gradient. *Rheol. Acta* **2017**, *56*, 1007–1032. [CrossRef]

84. Dinkgreve, M.; Fazilati, M.; Denn, M.; Bonn, D. Carbopol: From a simple to a thixotropic yield stress fluid. *J. Rheol.* **2018**, *62*, 773–780. [CrossRef]